

Reversible Photoinduced Electron Transfer in a Ruthenium Poly(2-methoxyaniline-5-sulfonic acid) Composite Film

Lynn Dennany,^{†,‡} Peter C. Innis,^{*,†} Gordon G. Wallace,[†] and Robert J. Forster[‡]

Intelligent Polymer Research Institute and ARC Centre of Excellence for Electromaterials Science, University of Wollongong, Northfields Avenue, Wollongong NSW 2522, Australia, and Biomedical Diagnostics Institute, National Centre for Sensor Research, School of Chemical Sciences, Dublin City University, Dublin 9, Ireland

Received: May 13, 2008; Revised Manuscript Received: July 9, 2008

In situ electron spin resonance (ESR) studies have been performed on composite films consisting of a ruthenium tris(bipyridyl) complex and an inherently conducting polymer, poly(2-methoxyaniline-5-sulfonic acid) (PMAS). The composites were investigated under white light irradiation and potential control conditions to probe photoinduced electron transfer between the ruthenium metal center and the conducting polymer. PMAS exhibited a clear ESR signal, characteristic of the presence of mobile single spin polarons within the polymer structure. Irradiation of the PMAS in the presence of the ruthenium metal center resulted in the photo-oxidation of the Ru^{2+} to the Ru^{3+} state, as a result of which the PMAS ESR signal was replaced by a response typical of the Ru^{3+} salt. Upon removal of the illumination, reversible photo switching occurred. This reversibility makes these novel composites promising for applications in areas such as chemical sensors, light switching, and light harvesting devices.

Introduction

In recent times, the possibility of combining an inherently conducting polymer with a metal center has been investigated with a view to taking advantage of electronic communication between metal centers through the conjugated backbone of the polymer.¹ As such, π -conjugated metallopolymers have attracted increased attention because of their potentially widespread applications.^{2,3} The extensive delocalization of π -electrons is well-known to be responsible for the array of remarkable characteristics that such polymers exhibit.^{4–6} These properties include nonlinear optical behavior, electronic conductivity, and exceptional mechanical properties^{7,8} such as tensile strength and resistance to harsh environments.

Metallopolymers are an important class of materials whose unusual properties originate from the coupling of the chemical, electronic, and optical properties of the conjugated polymer backbone to those of the metal center. The interest in these materials is stimulated by their numerous promising applications in electronic and optoelectronic devices.^{9–12} One of the main focuses of this area of research has been the development of an understanding of the nature and extent of the electronic coupling between the metal and the conjugated polymer backbone.^{13,14} For example, polymers based on the benzimidazole moiety in particular have long been recognized for their useful engineering properties and resilience. The preferred method of synthesizing polymers based on benzimidazole is the condensation reaction between a carboxylic acid and an appropriate substituted phenyl ring in polyphosphoric acid.^{2,7} This approach is known to be significantly more reliable than older techniques such as high temperature melt reactions between diamines (for benzimidazoles) and acids or esters, and the interfacial polycondensation of diamines with acid chlorides.³ Other systems have also been

investigated for this type of enhanced communication between adjacent metal centers.^{6,13,15}

Photoionization and photoelectron transfer in heterogeneous systems have been extensively studied with respect to light energy storage systems and as photorewritable images utilizing polyaniline.^{16,17} Numerous systems involving ruthenium tris(bipyridyl) $[\text{Ru}(\text{bpy})_3]^{2+/3+}$ complexes have been investigated for photoinduced charge transfer reactions. The combination of conjugated polymers with these types of systems is a major focus within our work to date. The presence of the metal center affects the polymer backbone properties via its redox state and a combination of steric and inductive effects, and vice versa.¹⁴ The characterization of the electronic interactions between adjacent metal centers has been of particular interest. Recently, the communication between the metal centers and the π -conjugated backbone of the conducting polymer containing Ru^{2+} has been demonstrated.¹⁸ It has also been demonstrated that these metal centers can function as “electronic gates”, allowing charge to be inserted into the polymer at reduced potentials.¹⁹

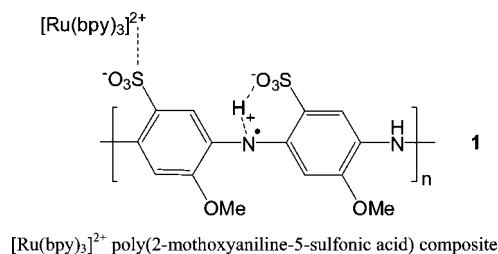
In this Article, we report on the photoinduced electron transfer between an inherently conducting polymer, poly(2-methoxyaniline-5-sulfonic acid) (PMAS), and a luminescent metal center within a surface confined structure. As seen in structure **1**, one of the dimeric sulfonic acid groups in the PMAS dimeric repeat unit is a self-doped radical cation N-center, while the other sulfonic acid is “free” and ionizes in aqueous solution to a SO_3^- sulfonate group, which can ionically bind to a $[\text{Ru}(\text{bpy})_3]^{2+}$ center. Electrochemical, photochemical techniques, as well as electron spin resonance spectroscopy (ESR) have been utilized to elucidate the mechanism of electron transfer between the metal center and the PMAS. Significantly, the production of a Ru^{3+} species through photo-oxidation without any external driving force was observed. These results indicate that there is considerable association between the luminescent metal center and the PMAS within the solid-state structure of a composite film and that electron transfer between these can be initiated photochemically. The reversible photoswitching also observed

* Corresponding author. Phone: +61 2 4221 3127. Fax: +61 2 4221 3114. E-mail: innis@uow.edu.au.

[†] University of Wollongong.

[‡] Dublin City University.

here for these composites highlights the considerable promise of these materials for applications in areas such as chemical sensors, light switching, and light harvesting devices.



Experimental Section

Apparatus. ESR spectra were recorded on a Bruker EMX ESR spectrometer under identical conditions: microwave frequency of 9.763 GHz, attenuator of 6.0 dB, sweep width of 700 G, modulation frequency of 100 kHz, modulation amplitude of 2 G, time constant of 327.68 ms, conversion time of 1310.72 ms, and sweep time of 1342.177 s were employed unless otherwise stated. Samples consisted of an electrochemically grown film of PMAS or a [Ru(bpy)₃]²⁺–PMAS composite on a Pt wire in aqueous electrolyte in a microwave cavity cell, electrochemical ESR flat cell (Wilma Glass), which ensures identical cell geometry and reproducible cavity tuning.

UV–vis absorbance spectra were recorded using a Shimadzu UV-240 spectrophotometer with spectral acquisition times of ca. 10 s. A Ru–PMAS composite-modified electrode was used as the working electrode with platinum gauze and Ag/AgCl as counter and reference electrodes, respectively. UV–vis spectra were acquired during photoillumination studies by turning off the excitation light source to acquire the spectra.

All other electrochemical experiments were carried out using a platinum wire as the working electrode in a conventional three-electrode assembly. Potentials are quoted versus Ag/AgCl, and all measurements were made at room temperature. Cyclic voltammetry analysis was made with a CH Instruments model 660 electrochemical analyzer.

Materials and Reagents. [Ru(bpy)₃]²⁺ was purchased from Sigma Aldrich as its chloride salt and used as received. PMAS emeraldine salt was prepared via the chemical synthesis method.²⁰ 2-Methoxyaniline-5-sulfonic acid (MAS) was provided by Mitsubishi Rayon, Japan, and purified by acid base crystallization before polymerization. All other reagents used were of analytical grade, and all solutions were prepared in milli-Q water (18 mΩ cm).

Composite Synthesis. Electropolymerization of the Ru–PMAS composite was performed by cyclic voltammetry over a potential range of –200 to 1300 mV, at a scan rate of 50 mV s^{–1} via in situ oxidation of the MAS in the presence of [Ru(bpy)₃]²⁺ and growth on subsequent cycles, for a minimum of 10 cycles. Electrosynthesis was performed in an electrolyte that contained 5 mM MAS monomer, pH 4.4, and 2 mM [Ru(bpy)₃]²⁺.¹⁸ Films were electrodeposited onto Pt, glassy carbon, or ITO-coated glass working electrodes. These modified electrodes were then washed (Milli-Q water) and allowed to dry overnight prior to analysis. Post-synthesis characterization was performed in aqueous 0.1 M H₂SO₄ unless otherwise stated. Surface coverage of the composite films, Γ, was determined by graphical integration of background corrected cyclic voltammograms (<5 mV s^{–1}). The surface coverages were approximately (7 ± 4) × 10^{–9} mol cm^{–2} unless otherwise stated. The resulting electrodeposited films were sparingly soluble in water due to the Ru

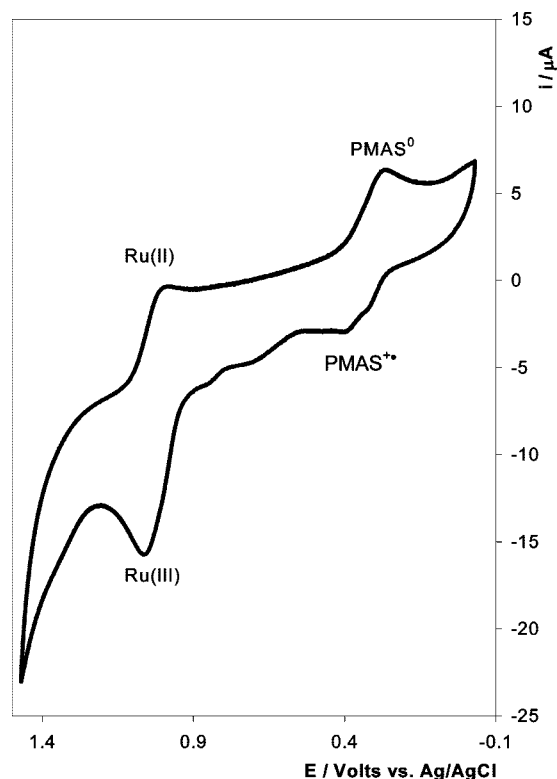


Figure 1. Typical cyclic voltammogram of an electrochemically grown composite film containing both [Ru(bpy)₃]²⁺ and PMAS on a platinum working electrode. Electrolyte was 0.1 M H₂SO₄, and a scan rate of 100 mV s^{–1} was used. The surface coverages were all ca. (5.4 ± 2) × 10^{–9} mol cm^{–2}.

complex cation ionically cross-linking the water-soluble PMAS polymer via the “free” sulfonic acid substituent (structure 1).

Results and Discussion

Electrochemical Properties of the [Ru(bpy)₃]²⁺–PMAS Composites. The electrochemical properties of the electrochemically grown Ru–PMAS films were investigated using cyclic voltammetry (Figure 1), displaying features typical of surface confined redox sites similar to those previously reported.^{18,20,21} Surface coverages were calculated by graphical integration of background corrected cyclic voltammograms (<5 mV s^{–1}) and were typically (7 ± 4) × 10^{–9} mol cm^{–2}. The formal potentials of both the Ru^{2+/3+} redox couple and those attributed to the different oxidation states of PMAS are similar to reported literature values.^{18,20,22} The anodic and cathodic peaks typical of a Ru^{2+/3+} couple were observed in all of the voltammograms at approximately 1050 mV.²³ At 0.8 V, the potential region below that of the oxidation of Ru²⁺ to Ru³⁺, the oxidation of the emeraldine salt form of PMAS to its pernigraniline base was observed as a small shoulder.

Under these nonilluminated conditions, the PMAS and Ru centers displayed independent redox functionality such that the redox waves observed for the composite can be assigned to charge localized on the metal centers and the π-conjugated polymer backbone, respectively. Significantly, the polymer backbone was not overoxidized in the potential region where the ruthenium metal center is oxidized, as is the case with previous systems involving ruthenium and conjugated polymers.¹⁴

Spectroscopic Analysis of the [Ru(bpy)₃]²⁺–PMAS Composite. As shown in previous investigations,^{24–26} the typical UV–vis spectrum of PMAS exhibited a band at 330 nm

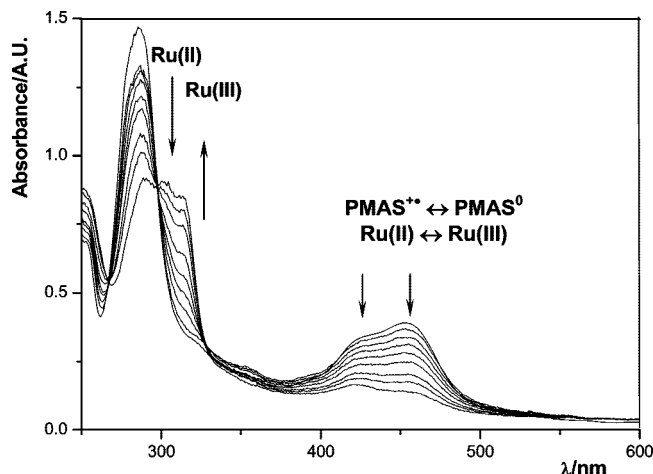


Figure 2. Spectral changes induced in a composite film of Ru-PMAS composite in 0.1 M H_2SO_4 with an incident light for a period of approximately 60 min. Arrows indicate the direction of the absorption band over time. Incident light was switched off during spectra accumulation, which took approximately 10 s. The surface coverages were all ca. $(6.7 \pm 2) \times 10^{-9} \text{ mol cm}^{-2}$.

attributed to $\pi-\pi^*$ transitions, and a sharp peak at 474 nm assigned as the lower wavelength polaron band. Reduction of PMAS to the leucoemeraldine form can be tracked by UV-vis spectroscopy, where the peaks of the original emeraldine salt form were replaced by a strong band at $\sim 405 \text{ nm}$ with a shoulder at $\sim 315 \text{ nm}$.^{20,22} Redox switching of the Ru centers can also be effectively tracked by UV-vis with strong bands at 345 and 460 nm typical of Ru^{2+} , while Ru^{3+} centers exhibit a strong band at 310 nm.²⁷

A typical response from an illuminated RuPMAS composite film on ITO-coated glass is shown in Figure 2. This spectrum contains the combined features of the $\text{Ru}^{2+/3+}$ species and the PMAS moiety. The spectro-chemical responses on ITO substrates were monitored over the shorter range of $300 \text{ nm} \leq \lambda \leq 600 \text{ nm}$ to confirm the production of a Ru^{3+} species at the potentials utilized throughout this investigation. The formation of the Ru^{3+} species was established by the decline of the peaks at 345 nm (which are metal-centered (MC) transitions)²⁷ and at 460 nm (which are MLCT bands from $d \rightarrow \pi^*$ transitions), indicative of Ru^{2+} centers. In addition, the appearance of a peak at about 310 nm was also characteristic of the Ru^{3+} species. Interestingly, these bands did not completely disappear, as would be expected for a $[\text{Ru}(\text{bpy})_3]^{2+}$ species.²⁷ This is most probably due to the competing reduction of the PMAS emeraldine salt to its leucoemeraldine form, which has strong bands at ca. 405 and 315 nm.^{20,24} The presence of these features effectively masks the decline of the Ru(II) UV-vis responses. The reduced form of the PMAS has been observed and reported in previous studies.²⁶

This trend could be improved by applying a potential bias, and this reduced the slower kinetics of the reoxidation of the leucoemeraldine to the emeraldine salt form of PMAS (typically an oxygen-driven process);^{28,29} however, this was not necessary to observe the photoinduced reaction. Notably, no redox spectral changes were observed with a +0.4 V bias in the absence of photoillumination.

ESR Properties of the $[\text{Ru}(\text{bpy})_3]^{2+}$ -PMAS Composites. Electron spin resonance is a very powerful method in the investigation of the fundamental conduction mechanisms of conducting polymers. The magnetic properties of PMAS originate from the presence of nonspin paired radical cations

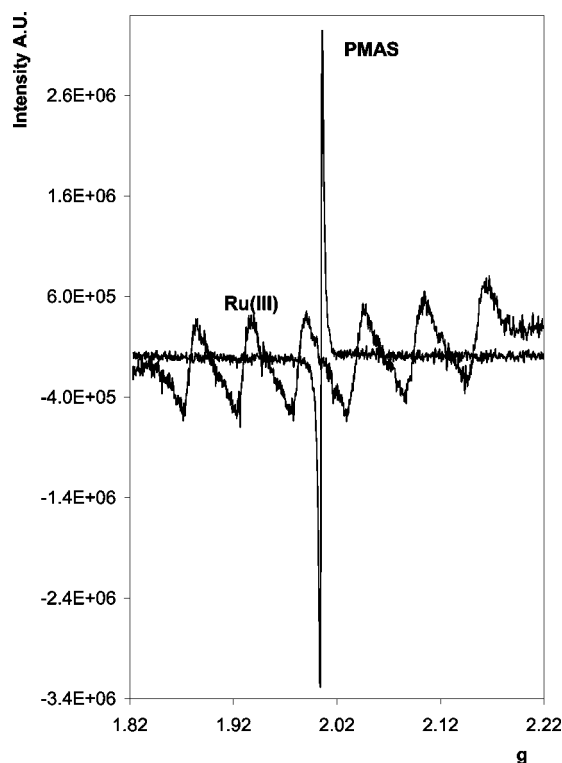


Figure 3. Typical ESR responses of an electrochemically grown film of PMAS on a Pt wire working electrode, and of a 10 mM $[\text{Ru}(\text{bpy})_3]^{2+}$ aqueous solution when the applied potential was held at $\sim 1.3 \text{ V}$ vs Ag/Ag^+ . A microwave frequency of 9.763 GHz, attenuator of 6.0 dB, sweep width of 700 G, modulation frequency of 100 kHz, modulation amplitude of 2 G, time constant of 327.7 ms, conversion time of 1310.7 ms, and sweep time of 1342.2 s were employed. The surface coverages were all ca. $(5 \pm 2) \times 10^{-9} \text{ mol cm}^{-2}$.

(polarons). The g factor for polyaniline and PMAS is typically around 2.003 and is common for heteroatom systems, indicating localization of spins at the nitrogen sites.^{14,28–30} A magnetic and charge transport study of PMAS by Lee et al.³¹ has shown that the density of states at the Fermi level, the density of Curie spin, and room temperature conductivity are all smaller than for partially (50–75%) sulfonated polyaniline (SPAN).³⁰ The larger twist of the phenyl rings and increased interchain separation induced by the methoxy side groups of PMAS and the higher density of sulfonate groups have been suggested as the origin of this lower density and conductivity, favoring the formation and stabilization of bipolarons, which are spin paired and therefore do not exhibit an ESR signal due to their spinless nature.

Typical ESR spectra of the solid-state electrochemically grown film of PMAS homopolymer and of solution-phase $[\text{Ru}(\text{bpy})_3]^{3+}$ are shown in Figure 3. PMAS exhibits an ESR singlet similar to that of polyaniline, with a g factor of ca. ~ 2.0045 g , and a line width (ΔG) of 3.483 G.²⁹ This g factor is consistent with previously obtained values for solution-phase PMAS samples and is consistent with the presence of electrons that are unpaired and delocalized primarily on phenyl rings, being ~ 2.0026 g for SPAN, as discussed above.³⁰ This is not to suggest that the electron may be delocalized over a single phenyl ring; the polarons have a significant spatial distribution in conjugated polymers. The spin density, however, is localized on particular sites, leading to changes in the g factor of different polymers.^{32,33} The observed g factor was close to the free electron value and in the range reported for various conducting polymers.¹⁴ However, this change in g factor accompanied with

a line broadening effect has been reported previously and has been ascribed to a spin-orbit coupling phenomenon induced by the presence of the coordinating metal center.¹⁴

The ESR signals for different ruthenium species are very different from that of the PMAS conducting polymer. An ESR signal could arise from several oxidation states of ruthenium, a low spin Ru^+ ($4d^6$) or a low spin Ru^{3+} ($4d^5$). Ru^0 ($4d^8$) or Ru^{2+} ($4d^6$) species do not give rise to ESR spectra. Figure 3 shows the ESR spectrum of a 1 mM solution of $[\text{Ru}(\text{bpy})_3]^{2+}$ generated by oxidizing Ru^{2+} to Ru^{3+} at 1.1 V in an electrochemical ESR flat cell (Wilma Glass). The observed spectrum was characteristic of the ESR signal of Ru^{3+} species. No ESR signal was observed for the Ru solution prior to application of a voltage, due to it being in the spinless 2^+ ground state.

The electrodeposited Ru-PMAS composite film retained the independent dark state electronic properties of the ruthenium complex and PMAS when in the ground state, with both reacting as expected at various applied voltages. Interestingly, the PMAS remained relatively stable at the higher potentials required to oxidize the $[\text{Ru}(\text{bpy})_3]^{2+}$ to $[\text{Ru}(\text{bpy})_3]^{3+}$ and was observed to be reversible over repeated cycling. Under these conditions, PMAS would be expected to be oxidized to the spinless pernigraniline state similar to previous studies on conjugated polymers with coordinated metal centers.^{14,16} In this Ru-PMAS composite film, the intensity of the Ru^{3+} ESR signal was markedly smaller than that of the conducting polymer. As a consequence, subsequent analysis of the composite film was optimized for the Ru^{3+} signal rather than the more intense PMAS response.

Previous studies by Lafalet et al. with different conjugated polymers did not observe the ESR signal of the Ru^{3+} species.¹⁴ This was attributed to the low stability of the polymer at the metal oxidation potential due to irreversible overoxidation of the matrix mediated by the Ru^{2+} species. Significantly, the Ru-PMAS composite films did not show this limitation observed for other conjugated metallopolymers.¹⁴ That is, the anodic potential scan was not restricted to the potential range corresponding to the backbone overoxidation.

An aqueous solution containing both the 10 mM $[\text{Ru}(\text{bpy})_3]^{2+}$ and the 0.05% w/v PMAS polymer was examined during and after photoirradiation by a halogen/deuterium light source. The solution was unaffected by the light, with the intensity and g factor of the PMAS signal remaining unchanged after prolonged exposure. Without photoillumination, the Ru-PMAS composite film reacted independently when under potential control. The application of a +0.4 V bias to a Ru-PMAS composite film on a Pt wire without photoillumination resulted in the decrease of the PMAS ESR response, eventually reaching a steady-state minimum after 20 min, presumably due to the formation of a mixed high spin polaron and spinless bipolaron system typical for a PMAS response (Figure 4).²⁶ Applying a bias of ~ 1.3 V vs Ag/AgCl at the working electrode without photoirradiating resulted in the emergence of the distinctive six-peaked Ru^{3+} ESR signal, similar to that in Figure 3, with the loss of the PMAS signal presumably due to the formation of spinless pernigraniline.

In sharp contrast, the ESR response for the Ru-PMAS composite film on a Pt wire electrode was very different when illuminated. Figure 5 illustrates the changes in the ESR signal of the composite film while under photoirradiation with a +0.4 V bias. Over time, the PMAS ESR signal was observed to decrease and was accompanied by the emergence of the six-peak Ru^{3+} ESR response. This result, coupled with the UV-vis observations seen in Figure 2, confirmed that electron transfer

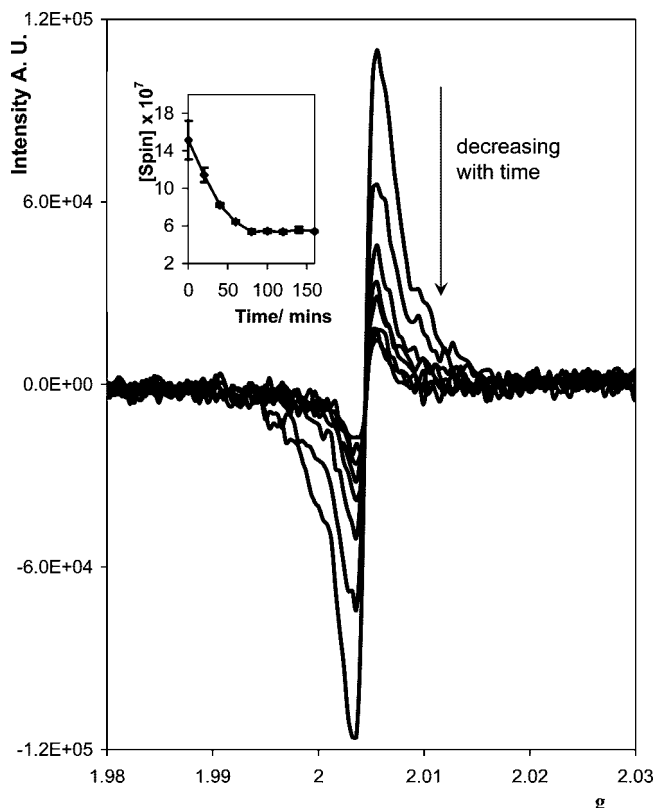


Figure 4. The ESR response of an electrochemically grown Ru-PMAS composite film on a Pt wire working electrode to an applied potential of 0.4 V vs Ag/Ag⁺ with no incident light penetrating the ESR cell over the same time scale as utilized in Figure 3. Electrolyte was 0.1 M H_2SO_4 . Microwave frequency of 9.763 GHz, attenuator of 6.0 dB, sweep width of 700 G, modulation frequency of 100 kHz, modulation amplitude of 2 G, time constant of 327.7 ms, conversion time of 1310.7 ms, and sweep time of 1342.2 s were employed. The surface coverages were all ca. $(5 \pm 2) \times 10^{-9}$ mol cm^{-2} . Inset shows the dependence of spin concentration as a function of time for the data illustrated in this figure.

occurred from the ruthenium species to the PMAS polymer. The eventual loss of the PMAS response was indicative of a reduction of the PMAS from the emeraldine salt to the spinless leucoemeraldine state, in contrast to the dark state observations. This result was distinctly different from the formation of the mixed polaronic/bipolaronic state that was observed for a solution-state mixture of PMAS and $[\text{Ru}(\text{bpy})_3]^{2+}$, as shown in Figure 4. Because the applied voltage was insufficient to oxidize the Ru^{2+} metal center to Ru^{3+} , an electron must therefore be transferred from the photochemically excited ruthenium species to the ground-state PMAS emeraldine salt, reducing it to the leucoemeraldine form.

The apparent electron transfer rate for this process was rather slow. This was evident from the gradual appearance of the Ru^{3+} signal, with ca. 1.5 h being required to completely oxidize the excited-state ruthenium species within the film. It is unclear if the slow rate is due to poor electrode kinetics or a series of competing back reactions. The reversal of the redox process was on a time scale similar to that of the forward reaction, suggesting that it was more likely due to poor kinetics rather than a back transfer process. However, this cannot be definitively concluded because some differences between the forward and reverse reaction may also result from leaching of the ruthenium metal center from the polymer, and as such no conclusion could be reached.

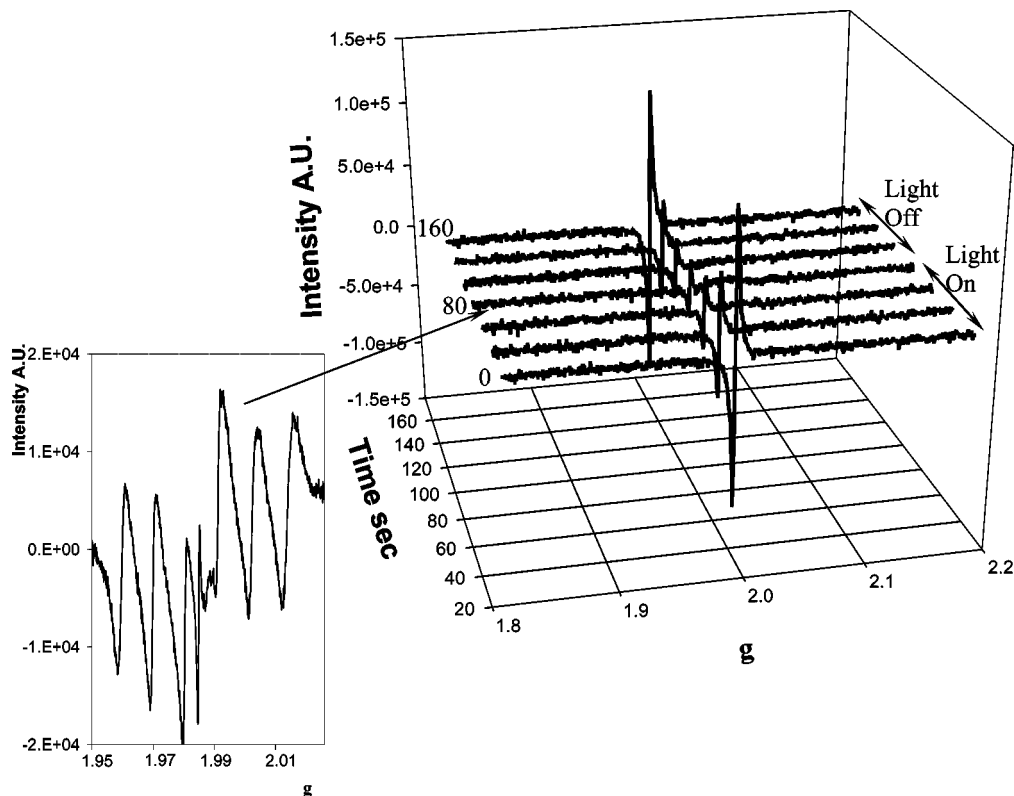
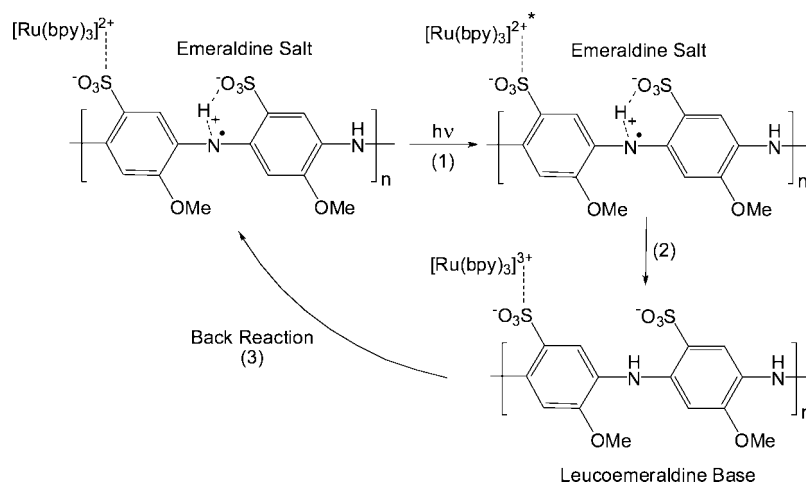


Figure 5. The photoinduced ESR response of an electrochemically grown Ru-PMAS composite film on a Pt wire working electrode without any applied voltage. The surface coverage was ca. $(5 \pm 2) \times 10^{-9}$ mol cm^{-2} . Electrolyte was 0.1 M H_2SO_4 . Microwave frequency of 9.763 GHz, attenuator of 6.0 dB, sweep width of 700 G, modulation frequency of 100 kHz, modulation amplitude of 2 G, time constant of 327.7 ms, conversion time of 1310.72 ms, and sweep time of 1342.2 s were employed. Inset shows the ESR response of the film prior to reaching steady state under photoillumination.

SCHEME 1: Proposed Reaction Mechanism for Photoinduced Electron Transfer within the Ru-PMAS Composite Films



Despite this, electron transfer does seem to be reversible because the PMAS signal returned accompanied by the disappearance of the Ru^{3+} signal once the light was switched off (Figure 5). This reaction was independent of any applied voltage and as such is unique. Even though a 0.4 V bias was utilized to keep the PMAS in the ES state, no voltage was needed to create the Ru^{3+} state, just incident light and close substituent proximity of the ruthenium complex and the PMAS. Clearly the application of a potential bias enhances the redox cycling process.

In contrast, independent solution-based studies resulted in no observable light-induced reaction. Given the known E^*_{ox} value of the oxidized ruthenium of -0.8 V, electron transfer is thermodynamically favorable, going “downhill” to the ground-

state PMAS backbone. The electron transfer process is explained in Scheme 1, with the back reaction (step 3) being sufficiently slow to allow the observation of the Ru^{3+} form in both the ESR and the UV-vis absorption spectra.

It cannot yet be determined whether the type of cycling shown in Scheme 1 is occurring in this system or if it is a more simple switching process, but clearly some form of back reaction (step 3) must be occurring given the slow electron transfer. Nonetheless, we have shown previously that an enhanced electron transport exists between the metal centers, resulting in increased rates of electron diffusion when compared to electronically isolated metallopolymers.¹⁸

Exact kinetic data for the back reaction cannot be obtained, as the Ru–PMAS composite film was unstable over the long time course of these experiments. Gradually over time the ruthenium complex was observed to dissolve out of the film matrix and into the solution, presumably as a result of the redox cycling process. It was also notable that once this occurred the $[\text{Ru}(\text{bpy})_3]^{2+}$ and PMAS species were no longer able to communicate with each other, resulting in the loss of the photoelectron transfer capability while retaining the same redox functionality. This suggests that for this type of electron transfer to occur the two species must be in direct contact with one another most likely due to ionic binding between the $[\text{Ru}(\text{bpy})_3]^{2+}$ and the anionic PMAS via the free SO_3^- groups on the polymer chain. Covalent binding of the metal center to the conducting polymer or the use of solvent systems in which PMAS and $[\text{Ru}(\text{bpy})_3]^{3+}$ are insoluble may improve the long-term stability of the composite.

Conclusions

Significantly, this contribution illustrated that irradiation of PMAS in the presence of a ruthenium metal center resulted in the photo-oxidation of the Ru^{2+} to Ru^{3+} state, observed as the PMAS ESR signal was replaced by a typical response of a Ru^{3+} salt. The phenomenon is extremely distance dependent and is only observed when the two compounds are interacting directly in the confined surface structure, presumably through ionic binding with the composite structure. This interaction can modulate both the electrochemical and the photophysical properties of the polymer and the ruthenium moiety, as shown in the ESR responses observed. Upon removal of the irradiation, the back reaction was observed.

These findings suggest a considerable number of possible applications of these composites including light harvesting and optical devices.

Acknowledgment. The financial support of Science Foundation Ireland under the Biomedical Diagnostics Institute (Award No. 05/CE3/B754) is deeply appreciated. The continued financial support from the Australian Research Council under the Centres of Excellence and QE(II) Fellowship (Innis) programmes is also greatly appreciated.

References and Notes

- (1) Cameron, C. G.; Pickup, P. G. *J. Am. Chem. Soc.* **1999**, *121*, 11773–11779.
- (2) Arnold, F. E. J.; Arnold, F. E. *Adv. Polym. Sci.* **1994**, *117*, 257.
- (3) Vogel, H.; Marvel, C. S. *J. Polym. Sci.* **1961**, *L*, 511.
- (4) Pickup, P. G. *J. Mater. Chem.* **1999**, *9*, 1641–1653.
- (5) Ochmanska, J.; Pickup, P. G. *J. Electroanal. Chem.* **1989**, *271*, 83–105.
- (6) Cameron, C. G.; Pickup, P. G. *Chem. Commun.* **1997**, *3*, 303–304.
- (7) Osaheni, J. A.; Jenekhe, S. A. *Chem. Mater.* **1992**, *4*, 1282.
- (8) Roberts, M. F.; Jenekhe, S. A. *Chem. Mater.* **1994**, *6*, 135.
- (9) Zhou, D.; Innis, P. C.; Wallace, G. G.; Shimizu, S.; Maeda, S.-I. *Synth. Met.* **2000**, *114*, 287–293.
- (10) Shimizu, S.; Saitoh, T.; Uzawa, M.; Yuasa, M.; Yano, K.; Maruyama, T.; Watanabe, K. *Synth. Met.* **1997**, *85*, 1337–1338.
- (11) Wei, X.-L.; Wang, Y. Z.; Long, S. M.; Bobeczko, C.; Epstein, A. J. *J. Am. Chem. Soc.* **1996**, *118*, 2545–2555.
- (12) Heeger, A. J. *J. Phys. Chem. B* **2001**, *105*, 8475–8491.
- (13) Cameron, C. G.; Pickup, P. G. *J. Am. Chem. Soc.* **1999**, *121*, 7710–7711.
- (14) Lafolet, F.; Genoud, F.; Divisia-Blohorn, B.; Aronica, C.; Guillerez, S. *J. Phys. Chem. B* **2005**, *109*, 12755–12761.
- (15) Zotti, G.; Schiavon, G.; Zecchin, S.; Berlin, A.; Pagani, G.; Canavesi, A. *Synth. Met.* **1996**, *76*, 255–258.
- (16) Kobayashi, N.; Fukuda, N.; Kim, Y. *J. Electroanal. Chem.* **2001**, *498*, 216–222.
- (17) Kim, Y.; Teshima, K.; Kobayashi, N. *Electrochim. Acta* **2000**, *45*, 1549–1553.
- (18) Dennany, L.; O'Reilly, E. J.; Innis, P. C.; Wallace, G. G.; Forster, R. *J. Electrochim. Acta* **2008**, *53*, 4599–4605.
- (19) Guillerez, S.; Kalaji, M.; Lafolet, F.; Novaes Tito, D. *J. Electroanal. Chem.* **2004**, *563*, 161–169.
- (20) Masdarolomoor, F.; Innis, P. C.; Ashraf, S.; Wallace, G. G. *Synth. Met.* **2005**, *153*, 181–184.
- (21) Dennany, L.; Forster, R. J.; Rusling, J. F. *J. Am. Chem. Soc.* **2003**, *125*, 5213–5218.
- (22) Masdarolomoor, F.; Innis, P. C.; Ashraf, S.; Kaner, R. B.; Wallace, G. G. *Macromol. Rapid Commun.* **2006**, *27*, 1995–2000.
- (23) Tokel, N. E.; Bard, A. J. *J. Am. Chem. Soc.* **1972**, *94*, 2862–2863.
- (24) Thorne, J. R. G.; Masters, J. G.; Williams, S. A.; Macdiarmid, A. G.; Hochstrasser, R. M. *Synth. Met.* **1992**, *49*, 159–165.
- (25) Kim, K.; Lin, L. B.; Ginder, J. M.; Gustafson, T. L.; Epstein, A. J. *Synth. Met.* **1992**, *50*, 423–428.
- (26) Innis, P. C.; Masdarolomoor, F.; Kane-Maguire, L. A. P.; Forster, R. J.; Keyes, T. E.; Wallace, G. G. *J. Phys. Chem. B* **2007**, *111*, 12738–12747.
- (27) Jurvis, A.; Balzani, V.; Barigelletti, F.; Campagna, S.; Belser, P.; Von Zelewsky, A. *Coord. Chem. Rev.* **1988**, *84*, 85–277.
- (28) Zhou, Q.; Zhuang, L.; Lu, J. *Electrochem. Commun.* **2002**, *4*, 733–736.
- (29) Sakharov, I. Yu.; Ouporov, I. V.; Vorobiev, A. Kh.; Roig, M. G.; Pletjushkina, O. Yu. *Synth. Met.* **2004**, *142*, 127–135.
- (30) Chen, S.-A.; Hwang, G.-W. *Macromolecules* **1996**, *29*, 3950–3955.
- (31) Lee, W.; Du, G.; Long, S. M.; Epstein, A. J.; Shimizu, S.; Saitoh, T.; Uzama, M. *Synth. Met.* **1997**, *84*, 807–808.
- (32) Kuroda, S.; Marumoto, K.; Ito, H.; Greenham, N. C.; Friend, R. H.; Shimoi, Y.; Abe, S. *Chem. Phys. Lett.* **2000**, *325*, 183–188.
- (33) Kuroda, S.; Marumoto, K.; Sakanaka, T.; Takeuchi, N.; Shimoi, Y.; Abe, S.; Kokubo, H.; Yamamoto, T. *Chem. Phys. Lett.* **2007**, *435*, 273–277.

JP804213R